JTTEE5 13:425-431
DOI: 10.1361/10599630419364
1059-9630/$19.00 © ASM International

Dependency of Fracture Toughness of Plasma Sprayed Al_2O_3 Coatings on Lamellar Structure

Chang-Jiu Li, Wei-Ze Wang, and Yong He

(Submitted October 12, 2002; in revised form February 1, 2003)

The fracture toughness of plasma-sprayed Al_2O_3 coatings in terms of critical strain energy release rate G_{Ic} was investigated using a tapered double cantilever beam (TDCB) approach. This approach makes the fracture toughness be measured only using the critical fracture load disregarding crack length during test. The Al_2O_3 coatings were deposited under different spray distances and plasma powers to clarify the effect of spray parameters on the G_{Ic} of the coatings. The fracture surfaces were examined using scanning electron microscope. On the basis of an idealized layer microstructure model for thermal sprayed coatings, the theoretical relationship between the cohesive fracture toughness and microstructure is proposed. The correlation between the calculated fracture toughness and observed value is examined. It was found that the fracture toughness of plasma sprayed Al_2O_3 coatings is not significantly influenced by spray distance up to 110 mm, and further increase in spray distance to 130 mm resulted in large decrease in the fracture toughness of the coatings. The G_{Ic} value predicted based on the proposed model using lamellar interface mean bonding ratio and the effective surface energy of bulk ceramics agreed well with the observed G_{Ic} data. Such agreement evidently shows that the fracture toughness of thermally sprayed ceramic coatings at the direction along coating surface is determined by lamellar interface bonding.

Keywords Al_2O_3, ceramic coating, fracture toughness, G_{Ic}, lamellar bonding ratio

1. Introduction

With the development of plasma spraying technology in the last several decades, thermally sprayed ceramic coatings have been successfully used in various industrial fields due to their excellent wear-resistance, thermal-resistance, and corrosion resistance, etc. When a thermal spray coating is used under a certain mechanical loading, the loading may cause the coating delaminating or spalling in service. This certainly leads to a decrease in coating effective thickness or even direct exposure of the substrate surface to operating environment. Many experiments revealed that the failure of the coating occurs easily from the interfaces between lamellae in the coating, for example, under localized load such as in abrasive wear,[1] or erosion,[2] and fracture mechanics test.[3-5]

The cohesive fracture along the interface between the lamellae in the coating implies that the fracture toughness of thermal spray coating depends much on lamellar bonding. Due to lack of quantitative data of microstructure, especially, the data on the lamellar structural parameters such as interface bonding and mean lamellar thickness, etc., the fracture behavior and fracture toughness values were explained only qualitatively based on the microstructure examination or apparent porosity in the coating. The comprehensive quantitative relationship between coating structure and fracture toughness has not been established. The recent development on the quantitative characterization of ceramic coating microstructure using structural parameters[6,7] has made it possible to clarify the relation between mechanical properties and microstructure of thermal spray coatings.[8] The correlations between microstructure and both Young's modulus[9] and erosion rate[10] established in previous studies confirmed that the layer structure of sprayed ceramic coating controls the mechanical properties. It is considered that the fracture toughness of thermally sprayed ceramic coatings depends also on the microstructure,[4,5,11] especially on the lamellar microstructural features of the coatings.

With regard to the measurement of coating toughness, the double cantilever beam (DCB) approach appears to be most widely used.[3,12-17] As to the standard uniform DCB specimen, because the compliance varies nonlinearly with crack length, it

Chang-Jiu Li, Wei-Ze Wang, and **Yong He,** State Key Laboratory for Mechanical Behavior of Materials, Welding Research Institute, School of Materials Science and Engineering, Xi'an Jiaotong University, Xi'an, Shaanxi, 710049, People's Republic of China. Contact e-mail: licj@mail.xjtu.edu.cn.

Nomenclature

F_c	critical load at which fracture occurs, N
B	crack width, mm
C	compliance of specimen at the point where load is applied, 10^{-3} mm N^{-1}
a	crack length, mm
u	displacement at the point where load is applied, mm
E	Young's modulus, GPa
x	distance along the crack plane measured from loading point, mm
h	beam height at the distance x, mm
G_{Ic}	fracture toughness, J m^{-2}
C_p	fracture path related constant
ν	Poisson's ratio
α	bonding ratio
γ_e	effective surface energy J m^{-2}

is required that the crack length be correctly and accurately determined for an accurate estimation of the fracture toughness in terms of critical strain energy release rate.[18] As to thermally sprayed coatings, however, McPherson et al. showed experimentally that the critical strain release rate of the coatings presents a dependency on crack length.[12-15] Therefore, it is certainly difficult to obtain accurate fracture toughness value for similar coatings with the DCB specimens. As for the measurement of critical strain energy release rate, Mostovoy et al. proposed a modified contoured DCB (CDCB) specimen.[18] The proper design of specimen configuration makes the compliance of the test piece be proportional to crack length. Consequently, the critical strain energy release rate, i.e., the fracture toughness, depends only on the critical load to the fracture during measurement. This approach makes the fracture toughness be measured only using the critical fracture load disregarding crack length during test.

Therefore, in the current study, to examine the dependency of fracture toughness of ceramic coatings on lamellar structure, the measurement of the fracture toughness was carried out using a tapered double cantilever beam (TDCB) approach, which was a simplified variation of CDCB test proposed by Mostovoy et al. The measurement was performed with the alumina coatings plasma-sprayed under different plasma powers and spray distances to reveal the dependency of the fracture toughness on the lamellar bonding comparing with previous results. Accordingly, a theoretical microstructural model for the fracture toughness of ceramic coating was proposed and correlation with experimental results was examined.

2. Experimental Procedures

2.1 Fracture Toughness (G_{Ic}) by the Tapered DCB Specimen

The TDCB approach for the measurement of the fracture toughness of ceramic coatings has been proposed elsewhere.[19] Simple description is given as follows. According to the theory of fracture mechanics, when using a DCB test the critical strain energy release rate, G_{Ic}, can be expressed as follows[20]:

$$G_{Ic} = \frac{F_c^2}{2B}\frac{\partial C}{\partial a} \quad \text{(Eq 1)}$$

Where F_c is the critical load at which fracture occurs, B the crack width, C the compliance of specimen at the point where load is applied, and a the crack length. Following Eq 1, the fracture toughness G_{Ic} is a function of $\partial C/\partial a$ besides the critical load and specimen geometry. For the DCB specimen, $\partial C/\partial a$ is also a function of crack length. This implies that the accurate crack length should be known for accurate measurement of G_{Ic}.

According to strength of materials, the compliance is the ratio of displacement to applied load:

$$u = CF \quad \text{(Eq 2)}$$

where u is the displacement at the point where load is applied. For the DCB specimen, the compliance C can be expressed as follows[21]:

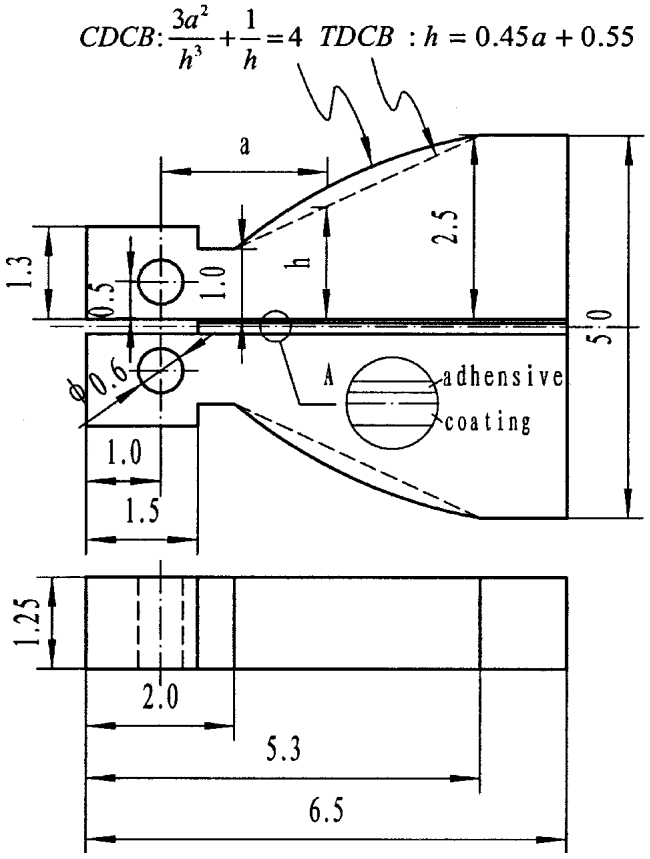

Fig. 1 Configuration and dimensions of the CDCB specimen[12] and the TDCB specimen (unit: cm)

$$C = \frac{24}{EB}\int_0^a \frac{x^2}{h^3}dx + \frac{6(1+\nu)}{EB}\int_0^a \frac{1}{h}dx \quad \text{(Eq 3)}$$

Where E is Young's modulus, ν is Poisson's ratio, x is the distance along the crack plane measured from loading point, and h the beam height at the distance x.

Referring to the approach proposed in Ref 18 and taking ν = 1/3, then, Eq 3 becomes

$$C = \frac{8}{EB}\int_0^a \left(\frac{3x^2}{h^3}+\frac{1}{h}\right)dx \quad \text{(Eq 4)}$$

Accordingly,

$$\frac{\partial C}{\partial a} = \frac{8}{EB}\left(\frac{3a^2}{h^3}+\frac{1}{h}\right) \quad \text{(Eq 5)}$$

Therefore, $\partial C/\partial a$ is the function of crack length and beam height at crack front for the DCB approach. Noticing that the beam height is not necessarily a constant and may be the function of crack length, following Mostovoy's proposal that the specimen is designed so that $\partial C/\partial a$ = constant, the G_{Ic} in Eq 1 is reduced to be the function of the critical load only. Such designed specimen was named as CDCB, as shown in Fig.1 sche-

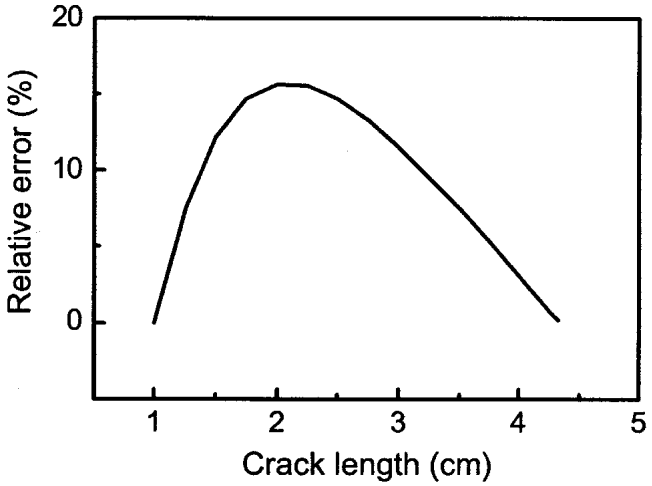

Fig. 2 Relative error of the beam height at crack tip in the TDCB specimen compared with that in the CDCB specimen against the crack length

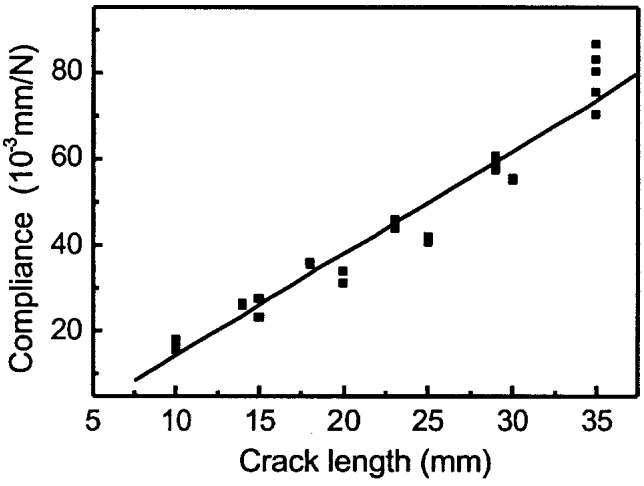

Fig. 3 Loading point compliance against crack length for the TDCB specimens; the solid line is obtained by the least square data fit

matically. In the current study, the contoured beam was machined into straight surface for the convenience of machining, which was referred to as the TDCB specimen. The dimensions of the specimen used in the current study are also shown in Fig.1. With the dimensions in the Fig. 1, the term in the parenthesis in Eq 5 becomes a constant 4. Due to the use of the straight line instead of a contoured curve, the error will occur to the $\partial C/\partial a$, which is a function of crack length. Solid line in Fig. 2 shows the relative error of the beam height at crack tip in the TDCB specimen compared with that in the CDCB specimen against the crack length. It can be found the maximum relative error of beam height is less than 16% when the TDCB specimen is used instead of the CDCB specimen.

2.2 Materials and Coating Deposition

The Al_2O_3 powder used was nominally commercially pure alumina, which had a particle size from 20-40 μm. Mild steel was used as substrate.

The Al_2O_3 coatings were deposited on the sandblasted surface to a thickness from 500 to 700 μm using a commercial plasma spray system (GP-80, Jiujiang Plasma Spray Factory, Jiujiang, China, 80 kW class). Argon was used as primary plasma operating gas and hydrogen was used as auxiliary gas. The pressures of both argon and hydrogen were operated at 0.7 and 0.4 MPa, respectively, during spraying. The flow of the primary gas was fixed to 47 l/min. Nitrogen was used as powder feed gas. Plasma jet was operated to deposit the coating at two power levels: 32.5 kW (650 A/50 V) and 39 kW (650 A/60 V). The deposition of the coatings was performed at four different spray distances: 70, 90, 110, and 130 mm, respectively, at two power levels. For each coating, at least six specimens were used for the fracture toughness measurement.

2.3 Fracture Toughness Test

In the present experiment, the contoured side of the beam was machined into straight surface and referred as the TDCB specimen. The dimensions of the specimen were shown in Fig.1. The width of the specimen was 12.5 mm. The TDCB specimen deposited with the coating was bonded to another coupling TDCB specimen without coating but with surface blasted using commercial adhesive (E-7, Shanghai Research Institute for Synthetic Resins, People's Republic of China). The curing of the adhesives was performed at 100 °C for 3 h. A pre-crack of 10-12 mm long with respect to the loading point was prepared through limiting the bonding of the coating to the coupling TDCB specimen by the adhesive. The test was performed using Instron 1195 (Canton, MA) type tensile tester (Load cells: 1 N to 100 kN, Crosshead speed range: 0.05-50 mm/min) at a crosshead speed of 5×10^{-5} m/min following the ASTM-E-399 standard. The loading and displacement of specimen were recorded simultaneously.

To ensure the accuracy of the test, only the specimen fractured in coating based on the examination of fractured surface was regarded as effective results, which were used to calculate the fracture toughness of the coating. The fractured surface was also examined using scanning electron microscopy (SEM) technique to examine the fracture behavior.

2.4 Calibration of Compliance

Ostojic and McPherson[12] have reported for the DCB test that the compliance tests on coated arms yielded the results identical to those for uncoated specimens. Based on those results, the test was performed with the specimens without coating for the calibration of compliance prior to the test of the deposited specimens in the current study. Two TDCB specimens, which were only blasted with alumina grit similar to coating process, were bonded together with the adhesives to give non-bonded area to a certain length from 10-35 mm as a pre-crack. The test was also performed following the ASTM-E-399 standard.

Figure 3 shows the relationship between compliance and crack length for the TDCB specimens used in the current study. The results yielded a reasonably linear relation between the compliance and crack length. The solid line shown in Fig. 3 represents the result obtained using least square fit technique which yielded the following correlation with a coefficient of 0.973 in the range of pre-cracks from 10-35 mm.

$$C = 2.369 \times 10^{-6}\, a - 9.25 \times 10^{-6} \quad \text{(m/N)} \qquad \text{(Eq 6)}$$

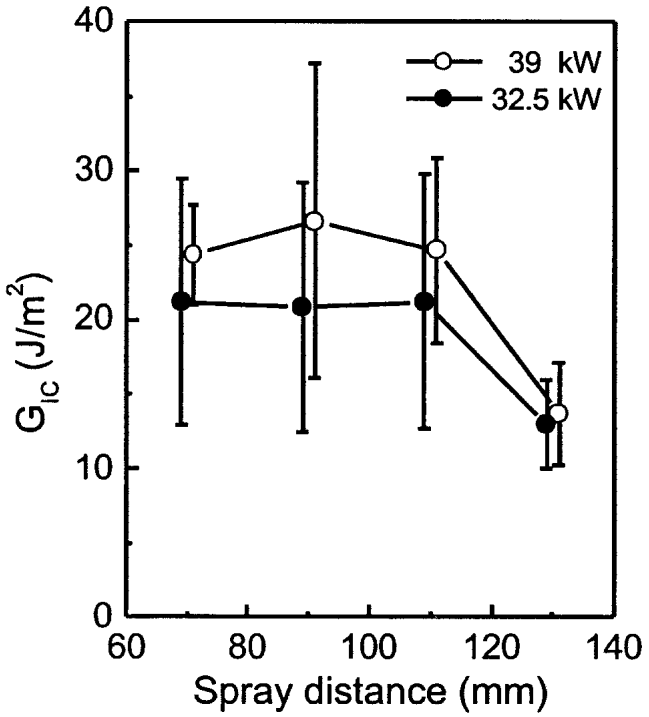

Fig. 4 Effect of spray distance on the mean critical strain energy release rate of plasma-sprayed Al_2O_3 coatings at plasma power of 39 and 32.5 kW

Accordingly, $\partial C/\partial a = 2.369 \times 10^{-6}$ (m/N). Taking width of specimen, i.e., width of crack, $B = 12.5$ mm, and substituting $\partial C/\partial a$ in Eq 1, for the present TDCB specimen,

$$G_{Ic} = 9.48 \times 10^{-5} F_c^2 \qquad (J/m^2) \qquad \text{(Eq 7)}$$

Accordingly, by measuring only the critical applied load at fracture, the fracture toughness G_{Ic} can be obtained with Eq 7.

3. Experimental Results

3.1 G_{Ic} Test Results

Figure 4 shows the effect of spray distance on the mean fracture toughness of Al_2O_3 coatings plasma-sprayed at two powers of 32.5 and 39 kW obtained by the TDCB approach. At plasma power of 39 kW, the coating yielded the mean fracture toughnesses of 24.4, 26.6, and 24.7 J/m^2 at spray distances of 70, 90, and 110 mm, respectively. It can be found that the fracture toughness of plasma sprayed Al_2O_3 coatings was not significantly influenced by spray distance up to 110 mm. When spray distance was increased to 130 mm, the mean fracture toughness of the coating was reduced remarkably to 13.7 J/m^2.

When the coatings were deposited at a power of 32.5 kW, a similar tendency of the fracture toughness on spray distance can be recognized with that observed at a power of 39 kW. The coatings yielded the mean fracture toughnesses of 21.1, 20.9, and 21.2 J/m^2 at spray distances of 70, 90, and 110 mm, respectively. Meanwhile, the mean fracture toughness of the coating deposited at spray distance of 130 mm was reduced to 13.0 J/m^2.

Berndt et al.[3,15] reported a mean fracture toughness of 12-28 J/m^2 for plasma sprayed Al_2O_3 coatings, which were determined using the uniform DCB specimen. It can be recognized that the present results agree well with the reported data despite the effect of spray conditions. Therefore, the present measurement using TDCB approach yielded reasonable results.

Compared with the G_{Ic} results of the coatings shown in Fig. 4, it can be found that plasma power presented limited influence on the fracture toughness of Al_2O_3 coatings at present power range, although a higher power was associated to a little high mean fracture toughness at spray distance less than 110 mm. Moreover, there is no significant influence of spray distance on fracture toughness of plasma sprayed Al_2O_3 coatings up to spray distance of 110 mm. When spray distance was increased from 110 to 130 mm, however, it was clearly found that the fracture toughness was decreased rapidly to a relatively low level.

The previous investigation of the microstructure of plasma-sprayed alumina coatings has revealed quantitatively the bonding ratio (the ratio of the total bonded area to the total apparent interface area) between lamellae in the coating and its dependency on plasma power and spray distance using copper plating approach.[22] Based on those results, it can be found that the bonding ratio reached to 32% under plasma conditions, which can melt substantial spray particles. The bonding ratio was also not changed for spray distance from 80 to 100 mm and dropped to a rather low level of about 17.8% when spray distance was increased to 150 from 100 mm. The present test results of coating fracture toughness yielded clearly the same dependency on plasma power and spray distance with those of lamellar bonding ratio. This fact means that fracture toughness of ceramic coating will be dominated by lamellar bonding in the coating.

3.2 Fracture Topography

Figures 5 and 6 show typical surface morphologies of fractured Al_2O_3 coatings compared with those of as-sprayed coatings deposited at two different spray distances under plasma power of 39 kW. The examination of fractured surface demonstrated that most fractured surface area presented a similar morphology to those of the as-sprayed coating surface. This implies that the cracks were preferable to propagate along the interface area between lamellae in the coating where there exists a great deal of non-bonded interface areas.[6,7] Such propagation of the cracking caused cohesive fracture. This fact has already been pointed out by previous investigation.[3] The similarity of the morphology of most fractured surface to that of the as-deposited splat confirmed that cohesive cracking occurs along the non-bonded interface areas. Therefore, it can be considered that the fracturing of the bonded areas between lamellae contributes primarily to the fracture toughness value of the coating.

On the other hand, the examination into fracture pattern also revealed that the fractured surface presented the terrace morphology. Such pattern suggests that cohesive cracking of ceramic coating occurs also through trans-lamellae through pre-existed vertical microcracks net[6,7] to accommodate an easily propagating route. However, since vertical cracks are mainly through-splat ones in one single individual lamella,[6] this fact suggested that the trans-lamellar propagation of the cracking would not increase the fracture toughness of the coatings significantly. The limited bonding at the interface area provides essen-

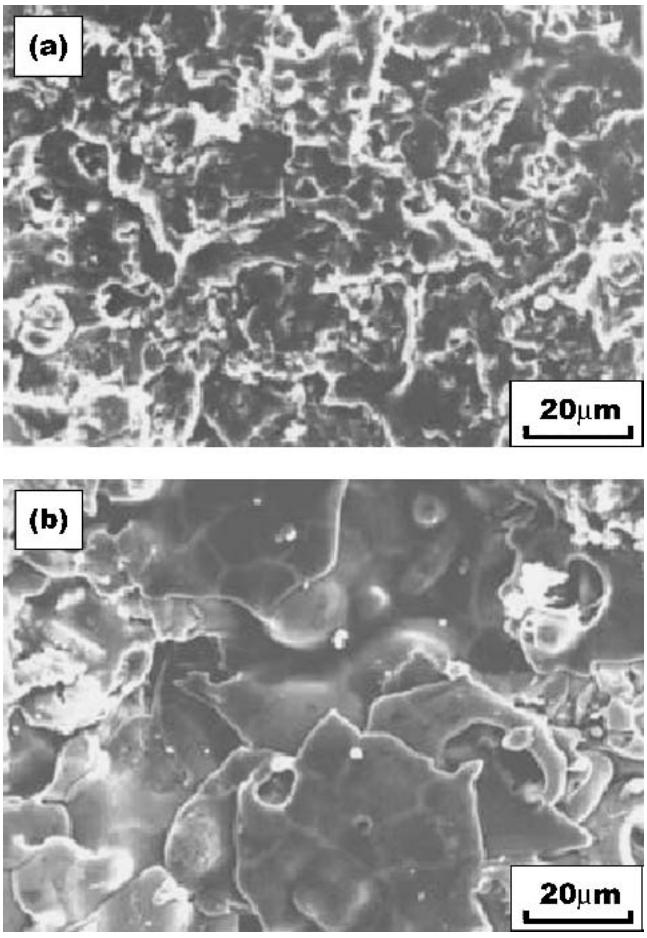

Fig. 5 Typical surface morphology of fractured Al_2O_3 coating compared with that of the as-sprayed coating at plasma power of 39kW and spray distance of 110 mm: **(a)** after fracture test, **(b)** as-sprayed

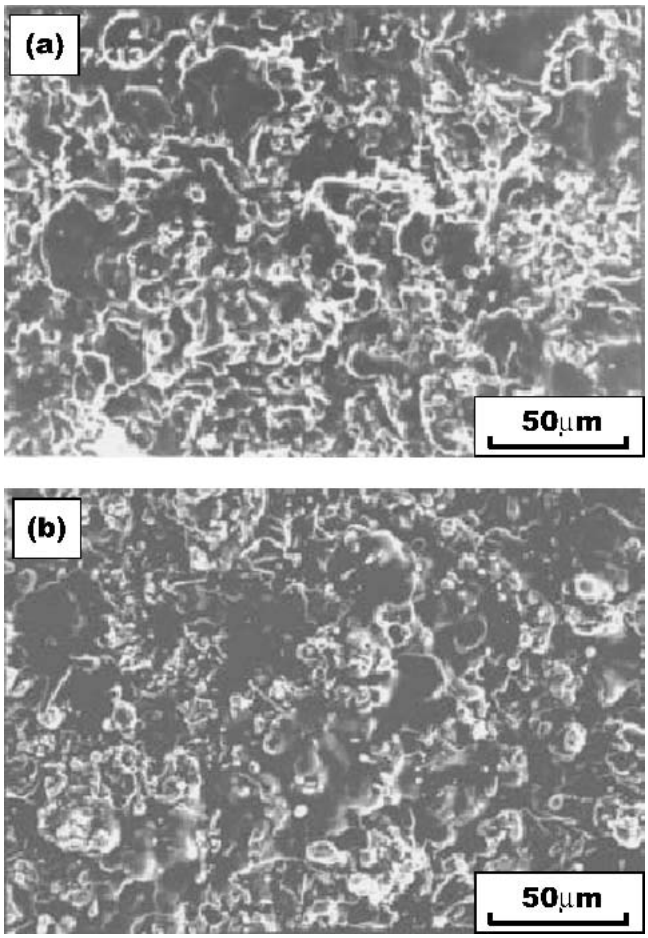

Fig. 6 Typical surface morphology of fractured Al_2O_3 coating compared with that of the as-sprayed coating at plasma power of 39kW and spray distance of 130 mm: **(a)** after fracture test, **(b)** as-sprayed

tially the gateway for crack to propagate through. Accordingly, the fracture toughness of spray coating will be dominated by lamellar bonding.

4. Relationship Between Lamellar Bonding and Fracture Toughness of Ceramic Coatings

4.1 Microstructural Model

Plasma sprayed ceramic coating presents a typical lamellar microstructure. The individual layers in the coating primarily have a quenched fine microstructure. However, it has been revealed that there exists only much limited bonding between lamellae.[6,23] Based on the examination by TEM[23] and visualization of detailed microstructure by using copper electroplating to alumina coating,[6] an idealized microstructure model for coating structure, as shown in Fig. 7, was proposed.[8] In such a model, the coating presents an ideal layered structure. The individual layers have the identical thickness. And the limited bonded areas are distributed between the adjacent layers. The total bonded interface fraction is defined as the bonding ratio (α), which is the ratio of the total bonded area to the total apparent interface area. At the non-bonded interface area, there exist interlamellar gaps, which can be considered as the pre-existed microcracks. Moreover, the vertical microcracks are usually observed in ceramic splat too.

4.2 Relationship Between Lamellar Bonding and Fracture Toughness of Thermal Spray Coating

For bulk ceramic materials, the critical strain energy release rate, i.e., fracture toughness (G_{Ic}) is generally expressed as[24]

$$G_{Ic} = 2\gamma_e \quad \text{(Eq 8)}$$

where γ_e is effective surface energy.

When a load is applied perpendicularly to layer direction of the sprayed coating with an ideal microstructure as shown in Fig. 7, the crack will be initiated from a nonbonded interface area and then propagated from the interfaces between lamellae in the coating. For such cohesive fracture of coating, G_{Ic} can be simply expressed by the following equation:

$$G_{Ic} = 2\ C_p\gamma_e\alpha \quad \text{(Eq 9)}$$

where C_p is a fracture path related constant, which depends on the tortuosity of flattened particle in thermally sprayed coating,

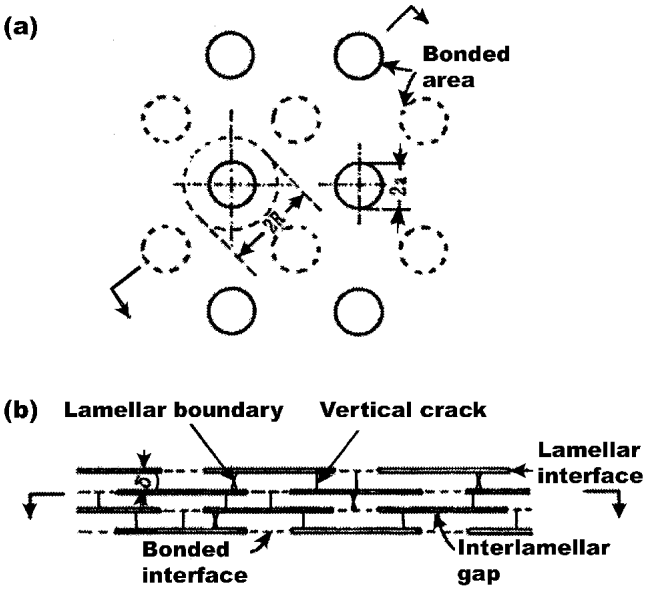

Fig. 7 Ideal model for the microstructure of thermally sprayed coating: **(a)** view of the plane parallel to lamellae plane, **(b)** view perpendicular to lamellar plane. The vertical cracks occur in the coating sprayed with brittle materials such as ceramics. For the coating sprayed with ductile metal the vertical cracks should be neglected.

i.e., the surface roughness of splat surface or deposited coating. For a coating consisting of well flattened particles, $C_p \approx 1$. Therefore, the fracture toughness in the direction along lamellae depends primarily on the bonding ratio between lamellae.

4.3 Correlation With Experimental Data

For sintered bulk Al_2O_3, γ_e varied from 25 to 45 J/m^2 as grain size was decreased from about 20 to less than 2 μm.[25] This yields a G_{Ic} of around 90 J/m^2 for bulk Al_2O_3 with fine grain structure of less than 2 μm based on the Eq 8.

Previous studies have quantitatively characterized the microstructure of plasma sprayed Al_2O_3 coatings using the structural parameters such as interface mean bonding ratio, mean lamellar thickness and vertical microcrack density.[6,7] According to those results, the bonding ratio between lamellae was influenced by spray parameters including spray distance and plasma power. The bonding ratio of the coating deposited under spray distance up to 100 mm was increased from 24% to a saturated level of about 32% with the increase in plasma power when using SG-100 spray gun. This means that for the optimized certain high plasma power level, the lamellar bonding does not change significantly. When the spray distance was increased from 100 to 150 mm, a rapid drop of the bonding ratio to 17.8% was observed. The present measurement results indicated clearly the similar dependency of fracture toughness on spray distance to that for the lamellar bonding ratio on spray distance reported previously[7] even though different spray systems were applied.

Taking account of the fine structure in individual splat in sprayed coating observed usually (for example, Ref 26) and bonding ratio data, using the proposed model (Eq 10), and taking C_p =1 and γ_e = 45 J/m^2, G_{Ic} value from 22 to 29 J/m^2 for spray distance up to 100 mm, and 14.7-16.2 J/m^2 at spray distances from 150 to 200 mm can be expected for α-Al_2O_3 coating.

Generally a thermally sprayed Al_2O_3 coating mainly consists of γ-Al_2O_3.[26] Although the data of effective surface energy of γ-Al_2O_3 is not available, it may be expected to be only a little lower than that of α-Al_2O_3. Although the practical fracture of the coating from lamellae occurs trans-lamellae through vertical cracks in a splat, compared the calculated values from the bonding ratio to the observed results mentioned above, it can be found that the observed G_{Ic} is well consistent with the calculated ones from the interface bonding ratio. Therefore, the relationship proposed in the current study between the fracture toughness and lamellae bonding ratio for plasma sprayed ceramic coatings represents well the dependence of fracture toughness of thermally sprayed coating on its microstructural feature. Accordingly, the fracture toughness of the coating along the lamellar direction can be reasonably predicted when the effective surface energy of individual splats and the bonding ratio between splats are known.

4.4 Effect of Spray Parameters on Coating Toughness

Generally, the properties of a thermal spray coating depend on its microstructure, which is determined by spraying conditions. The present results demonstrated clearly that G_{Ic} of plasma-sprayed Al_2O_3 coatings varied with plasma power and spray distance. The good correlation between the observed G_{Ic} and that estimated by the lamellar bonding ratio based on the model mentioned above indicates that the influence of spray conditions on G_{Ic} effects through the lamellar bonding ratio.

Kingery et al. reported that an increase in sintering temperature will raise the consolidation rate significantly.[27] The contact angle of molten metals on cemented tungsten carbides decreased very rapidly with the increase in temperature of molten metal when there were wetting phases to molten metal in the cemented carbides.[28] Therefore, it would be reasonable to consider that a high temperature of a spray particle prior impact on substrate results in a high mean bonding ratio between lamellae in the coatings. According to the influence of plasma power on the particle temperature and velocity during plasma-spraying, a certain plasma power, say, about 22 kW, is necessary to melt most powders[29] although it can be considered that this power level depends on spray gun design. Accordingly, the increase in plasma power results in an increase in particle velocity and little change in particle temperature. The effect of increase in power input on particle heating is to increase the number of particles, which are completely molten with little change in the mean temperature near the melting point. Therefore, when the power increased from 32.5 kW to 39 kW it can be considered that the mean particle temperature increased little, which resulted in little change of the mean bonding ratio. Consequently, the G_{Ic} showed no significant change under the present power conditions. On the other hand, the investigation into the influence of spraying distance on the distribution of mean particle temperature showed that when spray distance increased from 120 to 140 mm, the particles of mean temperature lower than the melting point increased substantially.[29] The previous study of the lamellar bonding ratio of plasma-sprayed Al_2O_3 coating revealed an abrupt drop when spray distance was changed from 100 to 150 mm. The present measurement results indicated clearly the similar dependency of fracture toughness on spray distance to

that of the lamellar bonding on spray distance reported previously,[22] even though different spray systems were applied. Therefore, the fracture toughness of spray coating at the direction along coating surface is determined by the mean bonding ratio between lamellae, which is influenced by spray conditions.

5. Conclusions

The effect of plasma power and spray distance on the fracture toughness of plasma sprayed Al_2O_3 coatings was investigated using a TDCB approach. This approach has an advantage of measuring the fracture toughness of the coating by only using fracture load without knowing the crack length at the fracture compared over the standard DCB approach. The measurement by the TDCB approach yielded the mean fracture toughness G_{Ic} from 13 to 27 J/m^2. These data were consistent well with those reported previously in the literature using standard uniform DCB specimen.[3]

It was found that spray distance did not influence significantly the fracture toughness of plasma sprayed Al_2O_3 coatings up to 110 mm. However, a further increase of spray distance from 110 to 130 mm resulted in a large decrease in the G_{Ic} of the coatings despite plasma power. This tendency was consistent with the dependency of the interface mean bonding ratio on spray distance reported previously.[7]

On the basis of the idealized layer microstructure model for thermal spray coating, the relation between cohesive fracture toughness along lamellar direction and interface bonding was proposed. The fracture toughness predicted based on the model using lamellar interface mean bonding ratio and the effective surface energy of bulk ceramics exhibited the reasonably good agreement with the observed G_{Ic} data. It was clear that the cohesive fracture toughness of thermally sprayed ceramic coating is determined by the interface bonding between lamellae. Due to the anisotropic characteristics of layer structure, the present model proposed is applied where the stress is perpendicular to the layer plane.

Acknowledgment

The present programmer was financially supported by Trans-Century Training Programmer Foundation for Talent of Chinese Education Ministry of China.

References

1. L.W. Crane, C.L. Johnston, and D.H. James: "Effect of Processing Parameters on the Shear Adhesion Strength of Arc Sprayed Deposits," in *Proc. 10th Int. Thermal Spraying Conf.*, DVS, Germany Welding Society, Dusseldorf, Germany, 1983, pp. 46-50.
2. Y. Arata, A.Ohmori, and C-J. Li: "Basic Study on Properties of Plasma Sprayed Ceramic Coatings," *Trans. Jpn. Weld. Res. Inst.*, 1986, *15,* pp. 339-48.
3. C.C. Berndt and R. McPherson: "A Fracture Mechanics Approach to the Adhesion of Flame and Plasma Sprayed Coatings," in *Proc. 9th Int. Thermal Spraying Conf.*, D.J.H Zaat, ed., Nederlands Instituut voor Lastechnick, Hague, 1980, pp. 310-16.
4. G. Thurn, G.A. Schneider, H-A. Bahr, and F. Aldinger: "Toughness Anisotropy and Damage Behavior of Plasma Sprayed ZrO_2 Thermal Barrier Coatings," *Surf. Coat. Technol.*, 2000, *123,* pp. 147-58.
5. P.J. Callus and C.C. Berndt: "Relationship Between the Model II Fracture Toughness and Microstructure of Thermal Spray Coatings," *Surf. Coat. Technol.*, 1999,*114,* pp. 114-28.
6. A. Ohmori and C-J. Li: "Quantitative Characterization of the Structure of Plasma Sprayed Al_2O_3 Coating by Using Copper Electroplating," *Thin Solid Films*, 1991, *201,* pp. 241-52.
7. A. Ohmori, C-J. Li, and Y. Arata: "Influence of Plasma Spray Conditions on the Structure of Al_2O_3 Coatings," *Trans. Jpn. Weld. Res. Inst.*, 1990, *19,* pp. 259-70.
8. C-J. Li and A. Ohmori: "Relationship Between the Structure and Properties of Thermally Sprayed Coatings," *J. Therm. Spray Technol.*, 2002, *11*(3), pp. 365-74.
9. C-J. Li, A. Ohmori, and R. McPherson: "The Relationship Between Microstructure and Young's Modulus of Thermally Sprayed Ceramic Coatings," *J. Mater. Sci.*, 1997, *32,* pp. 997-1004.
10. C-J. Li, A. Ohmori, and Y. Arata: "Evaluation of the Lamellar Bonding of Ceramic Coating by Particle Erosive Test," in *Proc. 14th Int. Thermal Spray Conf.*, A. Ohmori, ed., High Temperature Society of Japan, Osaka University, Osaka, Japan, 1995, pp. 967-72.
11. R.J. Damani and P. Makroczy: "Heat Treatment Induced Phase and Microstructural Development in Bulk Plasma Sprayed Alumina," *J. Eur. Ceram. Soc.*, 2000, *20,* pp. 867-80.
12. P. Ostojic and R. McPherson: "Determining the Critical Strain Energy Release Rate of Plasma-Sprayed Coating Using a Double-Cantilever Beam Technique," *J. Am. Ceram. Soc.*, 1988, *71,* pp. 891-99.
13. G.N. Heintze and R. McPherson: "Fracture Toughness of Plasma-Sprayed Zirconia Coatings," *Surf. Coat. Technol.*, 1988, *34,* pp. 15-23.
14. G.N. Heintze and R. McPherson: "A Further Study of the Fracture Toughness of Plasma-Sprayed Zirconia Coatings," *Surf. Coat. Technol.*, *36,* 1988, pp. 125-32.
15. C.C. Berndt and P. Ostojic: "Strength Testing of Plasma Sprayed Coatings," in *Proceedings of International Symposium on Advanced Thermal Spraying Technology and Allied Coatings*, Japan High Temperature Society, Osaka University, Osaka, Japan, 1988, pp. 191-97.
16. D.Z. Guo and L.J. Wang: "Measurement of the Critical Strain Energy Release Rate of Plasma Sprayed Coatings," *Surf. Coat. Technol.*, 1992, *56,* pp. 19-25.
17. D.Z. Guo and L.J. Wang: "Study of Fracture and Erosive Wear of Plasma Sprayed Coatings," *J. Therm. Spray Technol.*, 1993, *2,* pp. 257-63.
18. S. Mostovoy, P.B. Crosley, and E.J. Ripling: "Use of Crack-Line-Loaded Specimens for Measuring Plane-Strain Fracture Toughness," *J. Mater.*, 1967, *2,* pp. 661-81.
19. C.-J. Li, W.Z. Wang, and Y. He: "Measurement of Fracture Toughness of Plasma Sprayed Al_2O_3 Coatings Using a Tapered Double Cantilever Beam Method," *J. Am. Ceram. Soc.,* 2003, *86,* pp. 1437-39.
20. G.R. Irwin: "Analysis of Stresses and Strains Near the End of a Crack Traversing a Plate," *J. Appl. Mech.*, *24,* 1957, pp. 361-64.
21. E.J. Ripling, S. Mostovoy, and R.L. Patrick: "Measuring Fracture Toughness of Adhesive Joints," *Mater. Res. Stand.,* 1964, *4,* pp. 129-34.
22. A. Ohmori, C.-J. Li, and Y. Arata: "The Structure of Plasma-Sprayed Alumina Coatings Revealed by Copper Electroplating," in *Proc. 4th National Thermal Spray Conf.*, T.F. Bernecki, ed., ASM International, Materials Park, OH, 1991, pp. 105-13.
23. R. McPherson and B.V. Shafer: "Interlamellar Contact Within Plasma-Sprayed Coatings," *Thin Solid Films*, 1982, *97,* pp. 201-04.
24. B.R. Lawn and R.T. Wilshaw: *Fracture of Brittle Solids,* Cambridge University Press, New York, NY, 1975, pp. 65.
25. L.A. Simpson: "Microstructural Considerations for the Application of Fracture Mechanics Techniques," in *Fracture Mechanics of Ceramics,* R.C. Bradt, D.P.H. Hasselman, and F.F. Lange, ed., Plenum Press, NY, 1974, pp. 567.
26. R. McPherson: "The Microstructure of Thermally Sprayed Coatings," in *Proceedings of International Symposium on Advanced Thermal Spraying Technology and Allied Coatings*, Japan High Temperature Society, Osaka University, Osaka, Japan, 1988, pp. 25-30.
27. W.D. Kingery, H.K. Bowen, and D.R. Uhlmann: *Introduction to Ceramics*, 2nd ed., Wiley-Interscience, New York, NY, 1976, p. 448.
28. T. Yamaguchi, K. Harano, and K. Yajima: "Spreading and Reactions of Molten Metals on and With Cemented Carbides," in *Surfaces and Interfaces in Ceramic and Ceramic-Metal Systems*, J. Pask and A. Evans, ed., Materials Science Research, Plenum Press, NY, 1981, Vol. 14, pp. 503.
29. A. Vardelle, M. Vardelle, R. McPherson, and P. Fauchais: "Study of the Influence of Particle Temperature and Velocity Distribution Within a Plasma Jet Coating Formation," in *Proc. 9th Int. Thermal Spraying Conf.*, D.J.H Zaat, ed., Nederlands Instituut voor Lastechnick, Hague, 1980, pp. 155-61.